POLITECNICO DI TORINO
Repository ISTITUZIONALE

Enhancing consistency of microphysical properties of precipitation across the melting layer in dual-frequency precipitation radar data

Original
Enhancing consistency of microphysical properties of precipitation across the melting layer in dual-frequency precipitation radar data / Mroz, K.; Battaglia, A.; Fridlind, A. M.. - In: ATMOSPHERIC MEASUREMENT TECHNIQUES. - ISSN 1867-8548. - 17:5(2024), pp. 1577-1597. [10.5194/amt-17-1577-2024]

Availability:
This version is available at: 11583/2990116 since: 2024-07-01T15:27:01Z

Publisher:
Copernicus Publications

Published
DOI:10.5194/amt-17-1577-2024

Terms of use:

This article is made available under terms and conditions as specified in the corresponding bibliographic description in the repository

Publisher copyright

(Article begins on next page)

01 September 2024

Meccanica (2024) 59:833–845
https://doi.org/10.1007/s11012-024-01789-z

Lumped parameters models for the stability analysis of rotors supported on gas bearings

F. Colombo · L. Lentini · T. Raparelli · A. Trivella

Received: 24 October 2023 / Accepted: 19 March 2024 / Published online: 25 April 2024
© The Author(s) 2024

Abstract In this paper different lumped parameters models are presented for the stability analysis of rotors supported on gas bearings. The analysis is carried out taking into account the damping and stiffness coefficients of journal bearings, calculated with the perturbation method. Lumped parameters models of different complexity are discussed for the description of the main rigid modes of the spindle. In case of symmetric systems, it is shown that the complexity of the model can be reduced by halving the number of the degrees of freedom. The analogy with the single mass approach is demonstrated. The considerations discussed in the paper are preliminary for the stability analysis of more complex systems, such as the ones with non-fixed bushes.

Keywords Aerostatic bearings · Perturbation method · Linearized stability

List of symbols

A	State space matrix
C	Damping matrix
F_{unb}	Unbalance force
G	Gyroscopic matrix
I	Transversal moment of inertia of the shaft
I_p	Polar moment of inertia of the shaft
L_1, L_2	Axial length of journal bearings
K	Stiffness matrix
M	Mass matrix
R	Gas constant
T	Temperature
c_{ij}	Damping coefficients of the air film in journal bearings
e	Residual static unbalance of the shaft
h	Radial air gap
k_{ij}	Stiffness coefficients of the air film in journal bearings
l_1, l_2	Axial distances between the shaft center of mass and the middle plane of journal bearings
m	Mass of shaft
m_{s}	Mass of shaft concentrated on bearings
n	Number of degrees of freedom
p	Pressure in journal bearings
q, q'	State vectors of generalized displacements
r	Radial coordinate
$x_{\mathrm{c}}, y_{\mathrm{c}}$	Shaft radial displacements in correspondence of journal bearings
λ	Eigenvalue
ϑ	Angle of rotation in plane xy respect to axis x
ϑ_x, ϑ_y	Shaft rotations around axes x and y
γ	Residual dynamic unbalance of the shaft
μ	Dynamic viscosity of air
ν	Perturbation frequency
η	Real part of the eigenvalue (damping)
ζ	Damping factor

F. Colombo (✉) · L. Lentini · T. Raparelli · A. Trivella
Department of Mechanical and Aerospace Engineering, Politecnico Di Torino, Turin, Italy
e-mail: federico.colombo@polito.it

ω Rotational speed
ω_d Damped frequency

1 Introduction

Gas bearings systems suffer from the so-called half speed whirl, which is a self-excited phenomenon which occurs at high rotational speeds [1]. It involves the increase of the radius of the rotor orbits until a possible crash of the rotor with the bearings. The onset of the half-speed whirl occurs when the rotational speed exceeds the stability threshold. This phenomenon can be studied with two alternative approaches: the so-called orbit method and the linearized coefficients method.

The first method solves the time dependent Reynolds equation (RE) coupled with the equations of motion of the rotor [2]. It takes into account the nonlinear effects in bearings, but it is time expensive and it is unsuitable for creating stability maps. Explicit or implicit schemes can be employed to solve the time marching problem. A noteworthy method is the Alternating Direction Implicit (ADI) scheme [3], which involves the solution of a tridiagonal system and is less costly than the implicit scheme which involves a penta-diagonal system.

The second method is based on the linearization of the bearings forces around a given operational point [4] and on the solution of the eigenproblem resulting from the rotor equations of motion [5, 6]. The linearized stiffness and damping coefficients are computed with the so-called perturbation method [7]. The improved version of the method, presented by the same author in [8], is useful for rotor-dynamics calculation of unbalance response and stability. The importance of this method was confirmed by other authors, which implemented it to carry out the stability analysis of gas bearings systems. In [9] it was employed to analyze the stability of a foil bearing and obtain stability maps, which typically show the stability threshold curve on a plot where a mass parameter is represented vs the bearing number. The classical perturbation method and an extended perturbation procedure incorporating the foil compliance explicitly were developed in [10]. The linearization method was used in [11] to compute the gas film coefficients for a high speed cryogenic turboexpander and in [12] for a heat pump turbocompressor. An interesting analysis of tilting pads is given in [13]. Many other works on the topic can be found in literature, such as [14–17]. The linearized coefficients method is more convenient from the computational point of view than the time advancing methods as the time needed to compute the linearized coefficients and evaluate the stability is much smaller than the time needed to solve the time dependent problem. Moreover, it is capable of providing a better knowledge about the underlying sources of instability, if compared with the orbit method. Stability charts can be easily plotted to show quantitatively how much the system approaches the stability threshold [6, 7, 18–20].

The stability evaluation is in most of cases carried out considering the so-called single-mass approach [21–23], which simplifies the complexity of the full rotor-bearings model and gives a first approximation of the stability threshold. Anyway, it is not evident in which cases this approach is more convenient and in which cases the full rotor model is to be preferred. To clarify this aspect, this paper shows the equivalence of the single mass approach with the simplified rotor models with 2 degrees of freedom (DOFS) and put in evidence in which conditions these models are no more accurate in predicting the stability threshold of the rotor-bearings system. In particular, it demonstrates that in case the bearings are not symmetrical with respect to the rotor center of mass, the single mass approach gives just a first estimation of the instability threshold. The error in the estimation of the onset speed increases the more unsymmetrical is the system.

In the introduction the linearized coefficients method to evaluate the stability of rotors supported on gas bearings is discussed in this paper. The full rotor model with four degrees-of-freedom (4 DOFs) system is presented, showing in which cases it is possible to reduce the number of DOFs and consider separately the cylindrical and the conical whirl motions. The 2 DOFs models are also compared with the single point-mass approach and the analogy between the two is demonstrated. Such considerations are preliminary for the stability analysis of more complex systems, such as the ones with non-fixed bushes.

1.1 The lumped parameters models

The dynamic equations of motion of the spindle considered rigid are considered in case of fixed bushings.

The bearings forces are linearized around the central shaft positions and the coefficients of stiffness and damping are collected in matrixes $[K]$ and $[C]$. The system dynamics is described by Eq. (1)

$$[M]\ddot{q} + ([G] + [C])\dot{q} + [K]q = F_{unb} \tag{1}$$

where $[M]$ and $[G]$ are the stiffness and the gyroscopic matrixes respectively, q is the state vector of the generalized displacements and F_{unb} is the vector of the actions due to the residual unbalance of the shaft.

Matrixes $[K]$ and $[C]$ depend on the linearized coefficients of the radial air films in journal bearings, which are frequency dependent.

1.2 Rigid rotor with 4 DOFs

The rigid rotor model with 4 DOFs involves all the radial degrees of freedom of the shaft. The axial degree of freedom is not considered as the axial mode and the radial modes can be considered decoupled in a first approximation; the thrust bearing is supposed to have a little influence on the whirl stability of the electro-spindle due to its small radius compared with the axial distance of the journal bearings. It is possible to consider two alternative versions of the generalized displacements vector: vector q involves both the radial displacement of the center of mass of the shaft and the rotations of the shaft axis around axes x and y:

$$q = \left[\ x_C\ y_C\ \ \vartheta_y\ -\vartheta_x\ \right]'$$

Vector q' involves the radial displacements of the shaft measured in the middle radial plane of the journal bearings:

$$q' = \left[\ x_{C1}\ y_{C1}\ \ x_{C2}\ y_{C2}\ \right]'$$

The following kinematic relationship is valid

$$q' = \begin{bmatrix} 1 & 0 & l_1 & 0 \\ 0 & 1 & 0 & l_1 \\ 1 & 0 & -l_2 & 0 \\ 0 & 1 & 0 & -l_2 \end{bmatrix} q \tag{2}$$

where l_1 and l_2 are the axial distances between the shaft center of mass and the middle plane of journal bearings, see Fig. 1. Notice that in general the system is not symmetric and distances l_1 and l_2 do not coincide.

In case q is used, the system is described by Eq. (1), while in case q' is used, by Eq. (3)

$$[M']\ddot{q}' + ([G'] + [C'])\dot{q}' + [K']q' = F_{unb} \tag{3}$$

The expressions of the matrixes and of the unbalance vector are reported in Appendix A1. It is worth noticing that in Eq. (1) the mass matrix is diagonal,

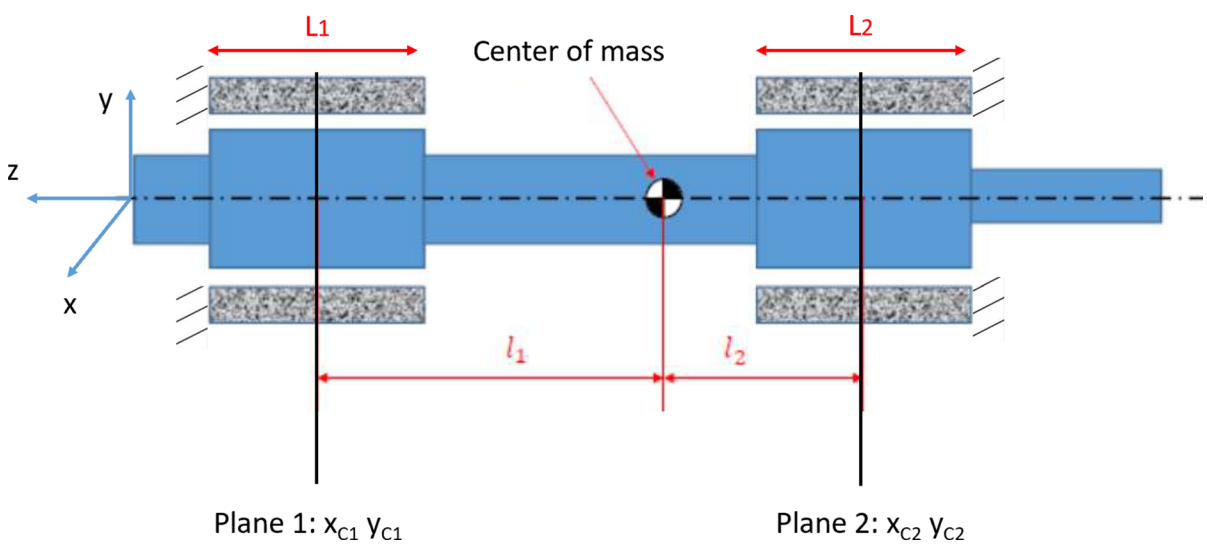

Fig. 1 Sketch of the system's geometry

while stiffness and damping matrixes are full. This means that in general the four equations are coupled. Similarly for system (2), in which also the mass matrix is not diagonal.

1.3 Rigid rotor with 2 DOFs, cylindrical mode

This model involves just the radial translation of the shaft, neglecting the tilting motions around axes x and y. The state vector is

$$q = \left[x_C \;\; y_C \right]'$$

The equations of motion in matrix form are

$$\begin{bmatrix} m & 0 \\ 0 & m \end{bmatrix} \ddot{q} + \begin{bmatrix} c_{xx1} + c_{xx2} & c_{xy1} + c_{xy2} \\ c_{yx1} + c_{yx2} & c_{yy1} + c_{yy2} \end{bmatrix} \dot{q} + \begin{bmatrix} k_{xx1} + k_{xx2} & k_{xy1} + k_{xy2} \\ k_{yx1} + k_{yx2} & k_{yy1} + k_{yy2} \end{bmatrix} q = me\omega^2 \begin{bmatrix} \cos \omega t \\ \sin \omega t \end{bmatrix} \tag{4}$$

where e is the radial distance between the shaft center of mass and the center of journals (residual static unbalance), m is the mass of the shaft and k_{ij} and c_{ij} the linearized coefficients of the air films.

1.4 Rigid rotor with 2 DOFs, conical mode

In this case only the rotation of the shaft axis around x and y fixed axes are taken into account, neglecting the radial motion of the center of mass of the shaft. The state vector is

$$q = \left[\vartheta_y \;\; -\vartheta_x \right]$$

The equations of motion in matrix form are

$$\begin{bmatrix} I & 0 \\ 0 & I \end{bmatrix} \ddot{q} + \left(\begin{bmatrix} 0 & I_p\omega \\ -I_p\omega & 0 \end{bmatrix} + \begin{bmatrix} c_{xx1} l_1^2 + c_{xx2} l_2^2 & c_{xy1} l_1^2 + c_{xy2} l_2^2 \\ c_{yx1} l_1^2 + c_{yx2} l_2^2 & c_{yy1} l_1^2 + c_{yy2} l_2^2 \end{bmatrix} \right) \dot{q} + \begin{bmatrix} k_{xx1} l_1^2 + k_{xx2} l_2^2 & k_{xy1} l_1^2 + k_{xy2} l_2^2 \\ k_{yx1} l_1^2 + k_{yx2} l_2^2 & k_{yy1} l_1^2 + k_{yy2} l_2^2 \end{bmatrix} q = \omega^2 \begin{bmatrix} (I - I_p)\gamma \cos \omega t \\ (I - I_p)\gamma \sin \omega t \end{bmatrix} \tag{5}$$

where I and I_p are the transversal and the polar moments of inertia of the shaft and γ is the angle between the principal axis of inertia and the rotational axis of the shaft (residual dynamic unbalance).

1.5 Computation of gas film coefficients

The stiffness and damping coefficients of the air films are computed with the so-called perturbation method. Starting from the static pressure distribution p_0, obtained solving the discretized Reynolds equation with finite difference technique, the dynamic pressure distribution Δp is obtained as a result of the sinusoidal perturbation Δx imposed to the shaft. As sketched in Fig. 2, the coefficients are both function of the rotational speed ω and the perturbation frequency ν.

The computation of such coefficients involves the solution of a linear system, resulting after discretization of the Reynolds equation in perturbed form (6):

$$\frac{1}{12\mu RT}\left[\oint_\Gamma p_0 h_0^3 \vec{\nabla} \Delta p \cdot \vec{n}\, d\Gamma + \oint_\Gamma h_0^3 \vec{\nabla} p_0 \cdot \vec{n} \Delta p d\Gamma - \oint_\Gamma 3 h_0^2 p_0 \Delta x \cos \vartheta \vec{\nabla} p_0 \cdot \vec{n}\, d\Gamma \right] - \frac{1}{RT} \oint_\Gamma \left(-p_0 \Delta x \cos \vartheta + h_0 \Delta p \right) \begin{bmatrix} \frac{\omega r}{2} \\ 0 \end{bmatrix} \cdot \vec{n}\, d\Gamma + G_p' \Delta p + G_x' \Delta x = \frac{j\nu}{RT} \iint_\Sigma \left(h_0 \Delta p - p_0 \Delta x \cos \vartheta \right) d\Sigma \tag{6}$$

Equation (6) represents a balance of flow in the perturbed condition; also the input flow through the supply orifices is considered in the balance, taking

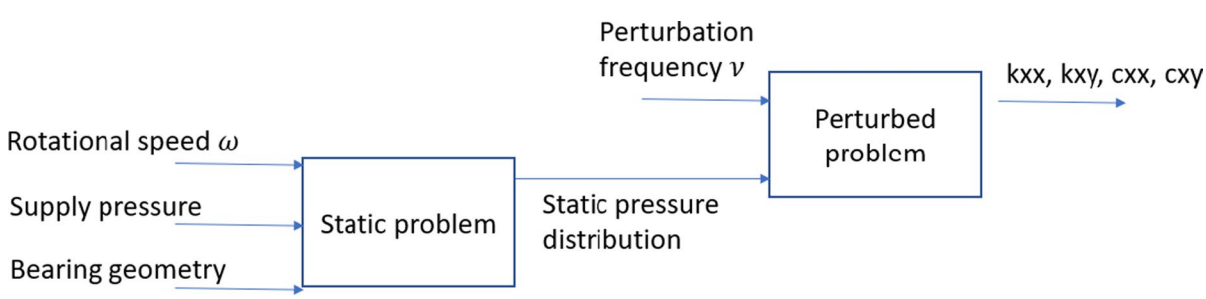

Fig. 2 Layout of the input and output variables involved in the static and in the perturbed problems

into account its partial derivatives with respect to pressure p (G_p') and x (G_x').

1.6 The Eigenvalue problem and the iterative procedure

The dynamic problem is written in the state space form, resulting in a linear system of size $2n$, where n is the number of DOFs:

$$\{\dot{x}\} = [A]\{x\}$$

$$\begin{Bmatrix} \dot{q} \\ \ddot{q} \end{Bmatrix} = \begin{bmatrix} 0 & I \\ -M^{-1}K & -M^{-1}C \end{bmatrix} \begin{Bmatrix} q \\ \dot{q} \end{Bmatrix} \tag{7}$$

The stability problem is faced calculating the eigenvalues of the state space matrix A. Complex eigenvalues appear in pairs, with conjugate imaginary parts:

$$\lambda = \lambda_r \pm j\lambda_i = \eta \pm j\omega_d \tag{8}$$

The real part represents damping, while the imaginary part the damped frequency. The natural frequencies and the damping factors of the modes are computed with:

$$\omega_n = \sqrt{\lambda_r^2 + \lambda_i^2}$$

$$\zeta = \frac{-\lambda_r}{\sqrt{\lambda_r^2 + \lambda_i^2}} \tag{9}$$

As the coefficients of the air films are frequency dependent, an iterative procedure is necessary to find the convergence between the damped frequency ω_d and the perturbation frequency ν. The following algorithm is thus implemented for each mode:

- Step1: k_{ij} and c_{ij} are evaluated at a first attempt frequency ν_0
- Step 2: the eigenvalues of system (3) are calculated, obtaining the damped frequency ω_d
- Step 3: k_{ij} and c_{ij} are evaluated at the new frequency $\nu = \omega_d$
- Step 4: in case the new frequency coincides with the damped frequency the algorithm has reached convergence, otherwise come back to step 2.

An example of the solution of the eigenvalue problem at different rotational speeds using this algorithm is given in Fig. 3; the damped frequency and the damping factors of the four modes are plotted vs the rotational speed considering the 4 DOFs model with fixed bushings. The negative damping factor of mode 4 indicates at which rotational speed the whirl becomes unstable (about $\omega_{th} = 130$ krpm). It is sufficient that one mode becomes unstable to have the unstable whirl.

2 Discussion

In this paragraph, it is shown how it is possible to simplify the 4 DOFs model if suitable conditions are verified. Three cases are considered:

(a) Different journal bearings (JBs) with unsymmetrical configuration
(b) Different JBs with symmetrical configuration
(c) Equal JBs with symmetrical configuration

It is shown that in the third case, in case the Coriolis terms are negligible, the equations of motion of translation and of rotation are uncoupled, so that it is possible to consider separately the cylindrical and the conical whirl motions in spite of considering the complete 4 dofs model. The bearings are supplied through two series of 10 supply holes of dia. 0.15 mm located at one fourth of the axial length. The radial film thickness is 20 μm. The rotor has mass $m = 230$ g, transversal moment of inertia $I = 453 \cdot 10^{-6}$ kg m^2 and polar moment of inertia $I_p = 14.9 \cdot 10^{-6}$ kg m^2.

2.1 Case a)

In this case, different JBs with unsymmetrical configuration are considered, see Table 1. The 4 DOFs model results are depicted in Fig. 3. The 2 DOFs cylindrical whirl model results are shown in Fig. 4 in the left, while the 2 DOFs conical whirl model results are shown in the right. The stability threshold obtained from the models are compared in Table 2.

By a comparison of the 2 DOFs models with the 4 DOFs model, the damped frequencies and the damping ratio of the modes do not coincide. The reason is that in this case the cylindrical and the conical whirl motions are coupled and the 2 DOFs models, which

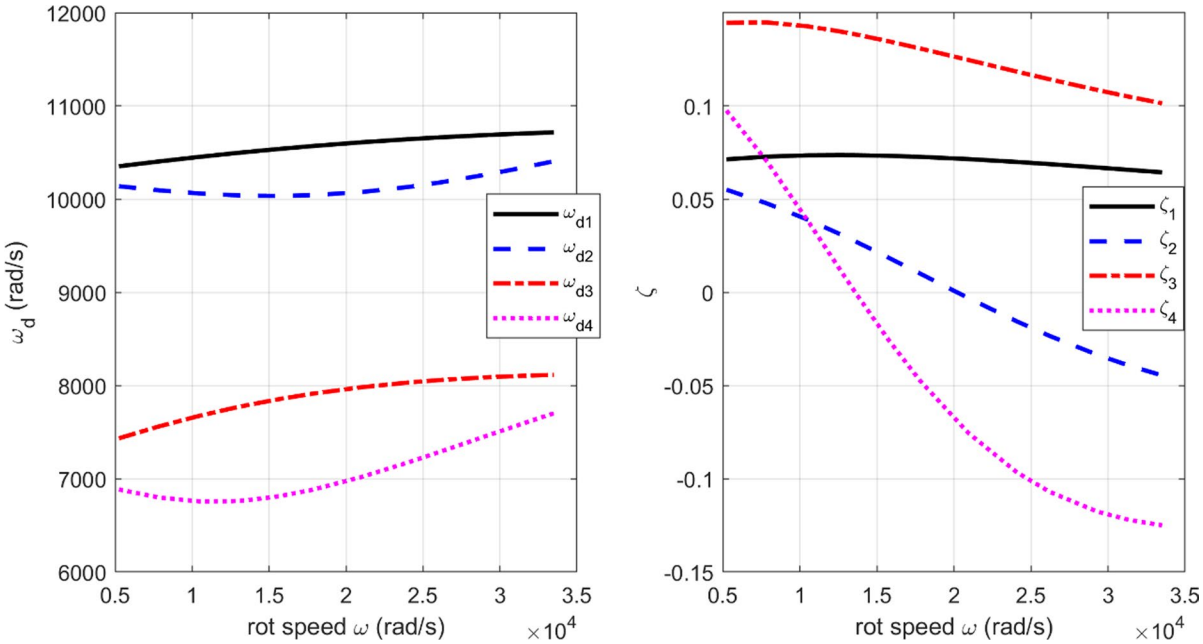

Fig. 3 Damped frequencies ω_d and damping factors ζ vs rotational speed; 4 DOFs model, case a)

Table 1 geometry considered in case a)

	Axial length (mm)	Distance from center of mass (mm)
Front bearing	$L_2 = 37$	$l_2 = 23$
Rear bearing	$L_1 = 26$	$l_1 = 64.6$

take into account only the pure cylindrical or the conical whirl, result to be inaccurate. The complete 4 DOFs model is to be preferred as it treats the coupled cylindrical and conical whirl.

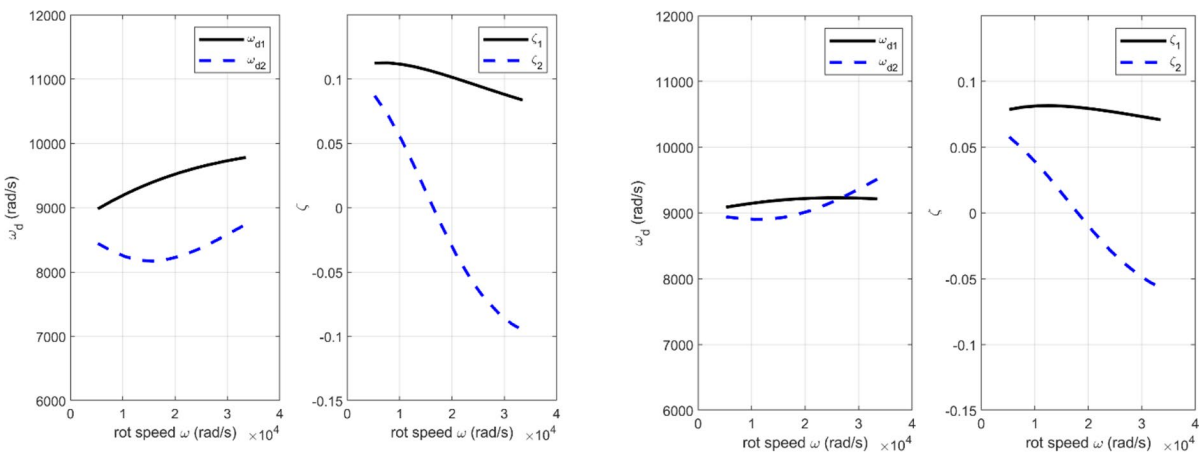

Fig. 4 Damped frequencies ω_d and damping factors ζ vs rotational speed for case a); 2 DOFs model, cylindrical whirl in the left; 2 DOFs model, conical whirl in the right

Table 2 comparison of the stability threshold according to the considered models; case a)

Model	Stability threshold (krpm)
2 DOFs cylindrical whirl model	16,420 rad/s≈157 krpm
2 DOFs conical whirl model	17,800 rad/s≈170 krpm
4 DOFs model	13,614 rad/s≈130 krpm

Table 3 geometry considered in case b)

	Axial length (mm)	Distance from center of mass (mm)
Front bearing	$L_2=37$	$l_1=l_2=43.8$
Rear bearing	$L_1=26$	

2.2 Case b)

In this case, different JBs with symmetrical configuration are considered, see Table 3.

The 4 DOFs model results are depicted in Fig. 5. The 2 DOFs cylindrical whirl model results are shown in Fig. 6 (left), while the 2 DOFs conical whirl model results are shown in the right. The stability threshold obtained from the models are compared in Table 4.

In this case the curves representing the damped frequency of the modes and the curves of the damping factor are more similar if the 4 DOFs model is compared with the 2 DOFs models. Due to the increased symmetry of the system, the 2 DOFs model give a better approximation of the 4 DOFs model with respect to case a). Anyway, the results do not yet coincide.

2.3 Case c)

In this case, equal JBs with symmetrical configuration are considered, see Table 5.

The 4 DOFs model results are depicted in Fig. 7. The 2 DOFs cylindrical whirl model results are shown in Fig. 8 in the left, while the 2 DOFs conical whirl model results are shown in the right.

The stability threshold obtained from the models are compared in Table 6, while Table 7 compares the stiffness and damping matrixes in the three cases. Stiffness coefficients are expressed in N/m, while damping coefficients in Ns/m. The table shows how matrixes $[K]$ and $[C]$ become band diagonal the more symmetrical the geometry becomes.

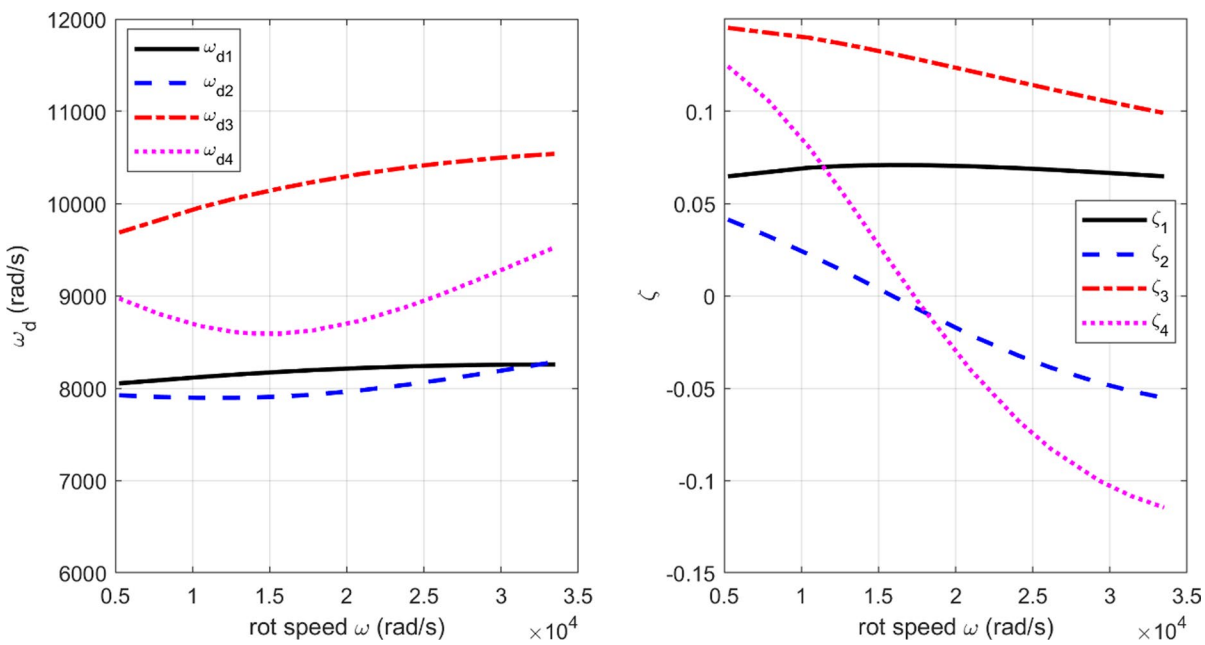

Fig. 5 Damped frequencies ω_d and damping factors ζ vs rotational speed; 4 DOFs model, case b)

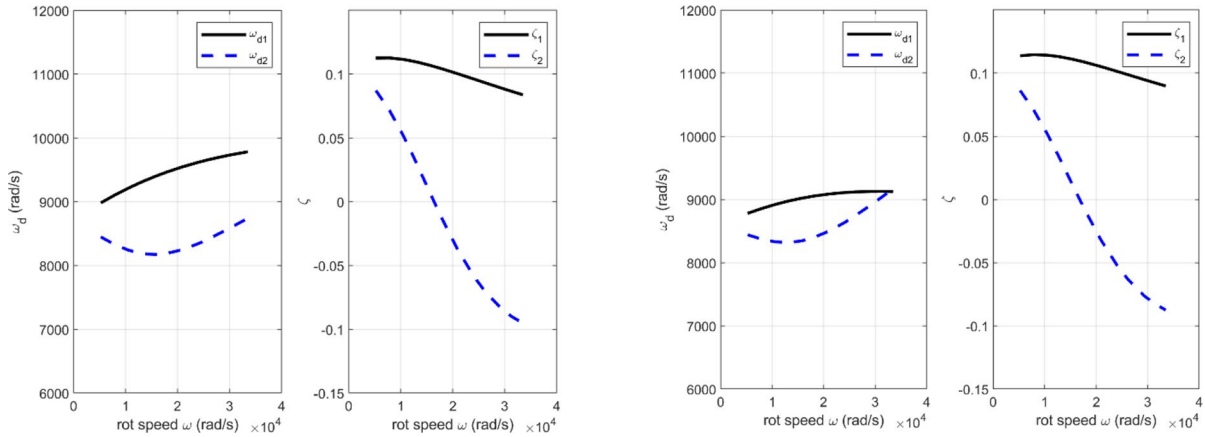

Fig. 6 Damped frequencies ω_d and damping factors ζ vs rotational speed for case b); 2 DOFs model, cylindrical whirl in the left; 2 DOFs model, conical whirl in the right

Table 4 comparison of the stability threshold according to the considered models; case b)

Model	Stability threshold (krpm)
2 DOFs cylindrical whirl model	16,430 rad/s≈157 krpm
2 DOFs conical whirl model	16,800 rad/s≈160 krpm
4 DOFs model	15,700 rad/s≈150 krpm

Table 5 geometry considered in case c)

	Axial length (mm)	Distance from center of mass (mm)
Front bearing	$L_1 = L_2 = 32$	$l_1 = l_2 = 43.8$
Rear bearing		

In this case, due to the complete symmetry of the journal bearings with respect to the center of mass of the shaft, the results of the 2 DOFs models perfectly match with the results of the 4 DOFs model. The curves representing the damped frequencies and the damping factors coincide.

The cylindrical and the conical motions are uncoupled in case the Coriolis terms are neglected and the system's geometry satisfies condition (10) or condition (11). In the first case there is perfect symmetry: distances l_1 and l_2 must coincide and the journal bearings must have the same geometry and the same radial film thickness (same air film coefficients):

$$\begin{cases} l_1 = l_2 \\ k_{ij,1} = k_{ij,2} \\ c_{ij,1} = c_{ij,2} \end{cases} \tag{10}$$

Condition (11) is more general, as the center of mass of the shaft could be not in the middle of bearings.

$$\begin{cases} k_{ij,1} l_1 = k_{ij,2} l_2 \\ c_{ij,1} l_1 = c_{ij,2} l_2 \end{cases} \tag{11}$$

This is evident from the stiffness and damping matrixes of the 4dofs model (see appendix A1) which reduce to band diagonal matrixes. For instance, in condition (10) $[K]$ is reduced into this form:

$$\begin{bmatrix} 2k_{xx} & 2k_{xy} & 0 & 0 \\ 2k_{yx} & 2k_{yy} & 0 & 0 \\ 0 & 0 & 2k_{xx}l^2 & 2k_{xy}l^2 \\ 0 & 0 & 2k_{yx}l^2 & 2k_{yy}l^2 \end{bmatrix} \tag{12}$$

It is thus demonstrated in which cases the full rotor model can be reduced: in case of complete symmetry (condition 10) or more in general according to condition (11). Of course, in case the system does not exactly satisfy such conditions but the asymmetry is small or condition (11) is almost

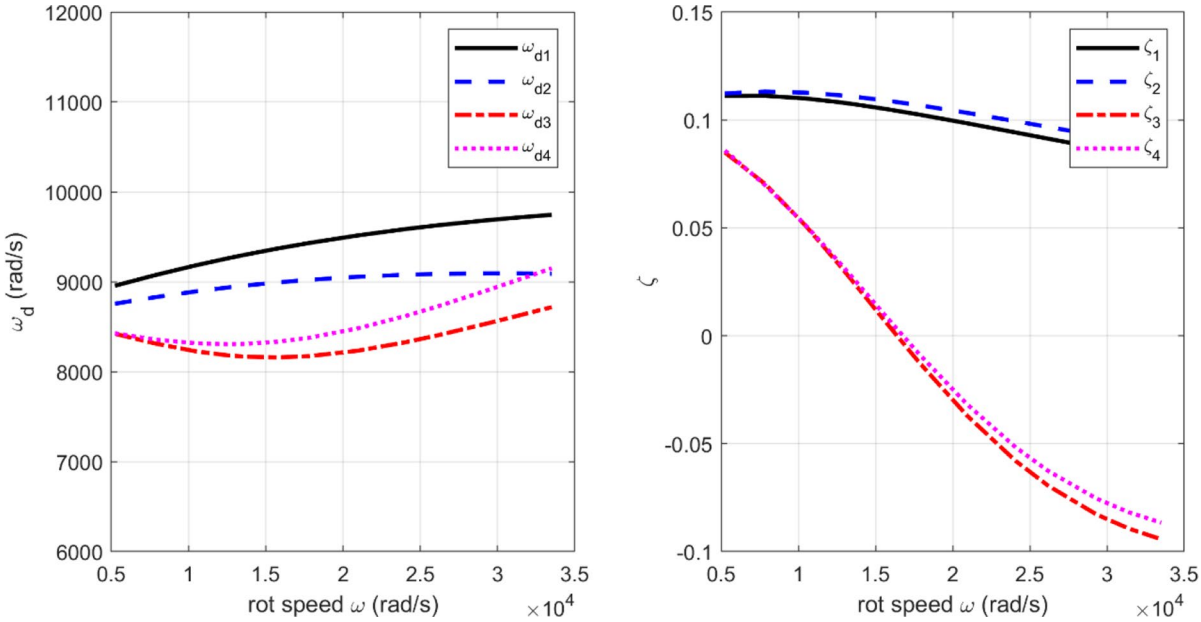

Fig. 7 Damped frequencies ω_d and damping factors ζ vs rotational speed; 4 DOFs model, case c)

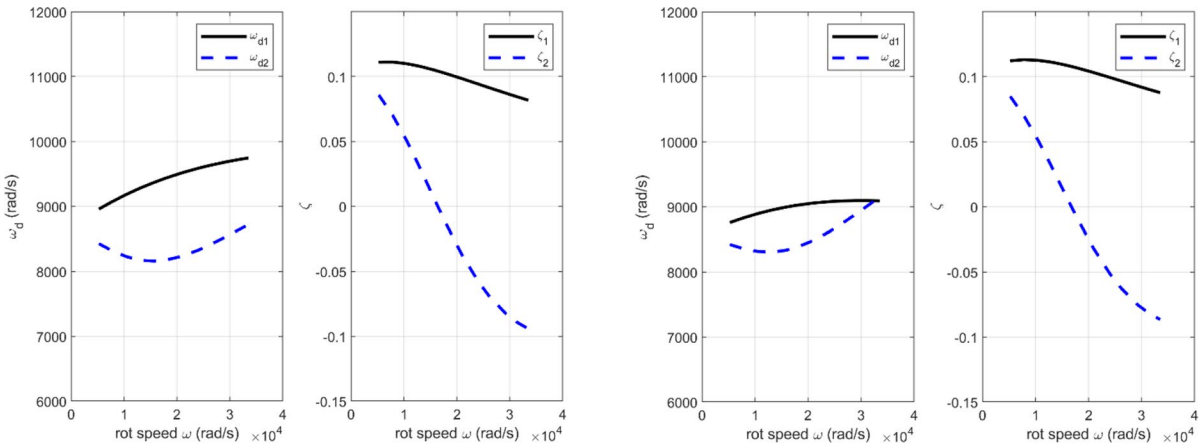

Fig. 8 Damped frequencies ω_d and damping factors ζ vs rotational speed for case c); 2 DOFs model, cylindrical whirl in the left; 2 DOFs model, conical whirl in the right

Table 6 comparison of the stability threshold according to the considered models, case c)

Model	Stability threshold (krpm)
2 DOFs cylindrical whirl model	16,400 rad/s≈156.7 krpm
2 DOFs conical whirl model	16,780 rad/s≈160 krpm
4 DOFs model	16,400 rad/s≈156.7 krpm

satisfied, the two modes can be still studied separately, being the out-of-diagonal elements negligible. In the other cases, the full model is to be preferred as it better estimates the stability threshold.

Table 7 comparison of matrixes [*K*] and [*C*] in cases a), b) and c)

case a)

K =

1.0e+07 *

1.8213	0.2423	0.0502	0.0101
-0.2423	1.8213	-0.0101	0.0502
0.0502	0.0101	0.0048	0.0008
-0.0101	0.0502	-0.0008	0.0048

C =

175.0444	-298.9556	6.9182	-13.5050
298.9556	175.0444	13.5050	6.9182
6.9182	-13.5050	0.5479	-1.0060
13.5050	6.9182	1.0060	0.5479

case b)

K =

1.0e+07 *

1.8213	0.2423	0.0123	0.0051
-0.2423	1.8213	-0.0051	0.0123
0.0123	0.0051	0.0035	0.0005
-0.0051	0.0123	-0.0005	0.0035

C =

175.0444	-298.9556	3.2773	-7.2868
298.9556	175.0444	7.2868	3.2773
3.2773	-7.2868	0.3358	-0.5735
7.2868	3.2773	0.5735	0.3358

case c)

K =

1.0e+07 *

1.8127	0.2366	0	0
-0.2366	1.8127	0	0
0	0	0.0035	0.0005
0	0	-0.0005	0.0035

C =

170.6080	-294.7607	0	0
294.7607	170.6080	0	0
0	0	0.3273	-0.5655
0	0	0.5655	0.3273

The coefficients are calculated with the perturbation method supposing $\omega = 200$ krpm and $\nu = 9000$ rad/s

2.4 The single mass approach

In literature the so-called single mass approach is known, which allows a quick estimation of the stability of rotor-bearings systems. As explained in [23, 24], the approach is quite common to perform the stability analysis of a rotor-journal bearings systems. According to this approach, the shaft mass is distributed in correspondence of the journal bearings considering a cylindrical motion or a conical motion. The masses m_{s1} and m_{s2} change in case the cylindrical or the conical whirl are considered, see Fig. 9.

Such expressions are compared with the masses that appear in [*M*'] in case a pure cylindrical or a pure conical motion are considered, see Appendix A2 for the detailed passages. It is thus demonstrated the analogy of the single mass approach with the simplified 2 DOFs models, in case of proper symmetry of the system.

3 Conclusions

This paper illustrates in details the linearized stability analysis of rotor-gas bearings systems. It shows in which cases a 4dofs rotor-bearings model can be simplified in a 2dofs model considering alternatively the cylindrical whirl or the conical whirl. In these cases the stability analysis can be carried out on each separate bearing concentrating on it a fraction of the shaft mass. The analogy of the reduced models with the so-called single mass approach is demonstrated. The models can be further extended to the stability analysis of gas bearings systems with non-fixed bushings.

Funding Open access funding provided by Politecnico di Torino within the CRUI-CARE Agreement.

Declarations

Conflict of interest The authors declare that the disclosed information is correct and that no other situation of real, potential or apparent conflict of interest is present.

Appendix A1: 4 DOFS MODEL

The matrixes of the 4 DOFs model of the rigid shaft are here explicitated. In case the generalized displacement vector *q* is used, the following expressions result:

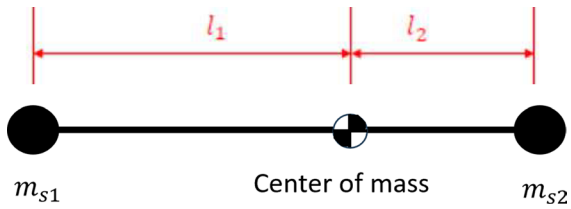

Fig. 9 Lumped masses in correspondence of journal bearings

$$
[M]=\begin{bmatrix} m & 0 & 0 & 0 \\ 0 & m & 0 & 0 \\ 0 & 0 & I & 0 \\ 0 & 0 & 0 & I \end{bmatrix}
$$

$$
[K]=\begin{bmatrix} k_{xx1}+k_{xx2} & k_{xy1}+k_{xy2} & k_{xx1}l_1-k_{xx2}l_2 & k_{xy1}l_1-k_{xy2}l_2 \\ k_{yx1}+k_{yx2} & k_{yy1}+k_{yy2} & k_{yx1}l_1-k_{yx2}l_2 & k_{yy1}l_1-k_{yy2}l_2 \\ k_{xx1}l_1-k_{xx2}l_2 & k_{xy1}l_1-k_{xy2}l_2 & k_{xx1}l_1^2+k_{xx2}l_2^2 & k_{xy1}l_1^2+k_{xy2}l_2^2 \\ k_{yx1}l_1-k_{yx2}l_2 & k_{yy1}l_1-k_{yy2}l_2 & k_{yx1}l_1^2+k_{yx2}l_2^2 & k_{yy1}l_1^2+k_{yy2}l_2^2 \end{bmatrix}
$$

$$
[G]=\begin{bmatrix} 0 & 0 & 0 & 0 \\ 0 & 0 & 0 & 0 \\ 0 & 0 & 0 & I_p\omega \\ 0 & 0 & -I_p\omega & 0 \end{bmatrix}
$$

$$
[C]=\begin{bmatrix} c_{xx1}+c_{xx2} & c_{xy1}+c_{xy2} & c_{xx1}l_1-c_{xx2}l_2 & c_{xy1}l_1-c_{xy2}l_2 \\ c_{yx1}+c_{yx2} & c_{yy1}+c_{yy2} & c_{yx1}l_1-c_{yx2}l_2 & c_{yy1}l_1-c_{yy2}l_2 \\ c_{xx1}l_1-c_{xx2}l_2 & c_{xy1}l_1-c_{xy2}l_2 & c_{xx1}l_1^2+c_{xx2}l_2^2 & c_{xy1}l_1^2+c_{xy2}l_2^2 \\ c_{yx1}l_1-c_{yx2}l_2 & c_{yy1}l_1-c_{yy2}l_2 & c_{yx1}l_1^2+c_{yx2}l_2^2 & c_{yy1}l_1^2+c_{yy2}l_2^2 \end{bmatrix} \tag{13}
$$

$$
F_{unb}=\omega^2\begin{bmatrix} me\cos\omega t \\ me\sin\omega t \\ (I-I_p)\gamma\cos(\omega t+\varphi_1) \\ (I-I_p)\gamma\sin(\omega t+\varphi_1) \end{bmatrix}
$$

In case the generalized displacement vector q' is used, the following expressions result:

$$
\begin{aligned}
[M'] &= \frac{1}{l_1+l_2}\begin{bmatrix} ml_2 & 0 & ml_1 & 0 \\ 0 & ml_2 & 0 & ml_1 \\ I & 0 & -I & 0 \\ 0 & I & 0 & -I \end{bmatrix} \\
[K'] &= \begin{bmatrix} k_{xx1} & k_{xy1} & k_{xx2} & k_{xy2} \\ k_{yx1} & k_{yy1} & k_{yx2} & k_{yy2} \\ k_{xx1}l_1 & k_{xy1}l_1 & -k_{xx2}l_2 & -k_{xy2}l_2 \\ k_{yx1}l_1 & k_{yy1}l_1 & -k_{yx2}l_2 & -k_{yy2}l_2 \end{bmatrix} \\
[G'] &= \frac{1}{l_1+l_2}\begin{bmatrix} 0 & 0 & 0 & 0 \\ 0 & 0 & 0 & 0 \\ 0 & I_p\omega & 0 & -I_p\omega \\ -I_p\omega & 0 & I_p\omega & 0 \end{bmatrix} \\
[C'] &= \begin{bmatrix} c_{xx1} & c_{xy1} & c_{xx2} & c_{xy2} \\ c_{yx1} & c_{yy1} & c_{yx2} & c_{yy2} \\ c_{xx1}l_1 & c_{xy1}l_1 & -c_{xx2}l_2 & -c_{xy2}l_2 \\ c_{yx1}l_1 & c_{yy1}l_1 & -c_{yx2}l_2 & -c_{yy2}l_2 \end{bmatrix}
\end{aligned} \tag{14}
$$

Table 8 expressions of the masses concentrated in correspondence to the journal bearings

	m_{s1}	m_{s2}
Cylindrical whirl	$m\frac{l_2}{l_1+l_2}$	$m\frac{l_1}{l_1+l_2}$
Conical whirl	$\frac{I}{l_1}\frac{1}{l_1+l_2}$	$\frac{I}{l_2}\frac{1}{l_1+l_2}$

Appendix A2: analogy with the single-mass approach

Cylindrical whirl

Starting from system (3) and imposing the cylindrical whirl it is.

$$
x_{C1}=x_{C2}=x_C;y_{C1}=y_{C2}=y_C;\gamma=0
$$

The system becomes

$$
\begin{aligned}
&\frac{1}{l_1+l_2}\begin{bmatrix} ml_2+ml_1 & 0 & 0 & 0 \\ 0 & ml_2+ml_1 & 0 & 0 \end{bmatrix}\begin{bmatrix} \ddot{x}_C \\ \ddot{y}_C \end{bmatrix} \\
&+\begin{bmatrix} k_{xx1}+k_{xx2} & k_{xy1}+k_{xy2} \\ k_{yx1}+k_{yx2} & k_{yy1}+k_{yy2} \\ k_{xx1}l_1-k_{xx2}l_2 & k_{xy1}l_1-k_{xy2}l_2 \\ k_{yx1}l_1-k_{yx2}l_2 & k_{yy1}l_1-k_{yy2}l_2 \end{bmatrix}\begin{bmatrix} x_C \\ y_C \end{bmatrix}=\omega^2\begin{bmatrix} me\cos\omega t \\ me\sin\omega t \\ 0 \\ 0 \end{bmatrix}
\end{aligned} \tag{15}
$$

where for brevity the damping matrix is not indicated as it has a structure similar to the stiffness matrix. In case of symmetry ($k_{ij1}\approx k_{ij2}$ and $l_1\approx l_2$, or more generally $k_{ij1}l_1\approx k_{ij2}l_2$) the last two lines are zeroed and the system becomes

$$
\begin{aligned}
&\begin{bmatrix} m_{s1}+m_{s2} & 0 \\ 0 & m_{s1}+m_{s2} \end{bmatrix}\begin{bmatrix} \ddot{x}_C \\ \ddot{y}_C \end{bmatrix} \\
&+\begin{bmatrix} k_{xx1}+k_{xx2} & k_{xy1}+k_{xy2} \\ k_{yx1}+k_{yx2} & k_{yy1}+k_{yy2} \end{bmatrix}\begin{bmatrix} x_C \\ y_C \end{bmatrix} \\
&=\omega^2\begin{bmatrix} (m_{s1}e_1+m_{s2}e_2)\cos\omega t \\ (m_{s1}e_1+m_{s2}e_2)\sin\omega t \end{bmatrix}
\end{aligned} \tag{16}
$$

where m_{s1} and m_{s2} are the masses in correspondence of bearings, see Table 8, and e1 and e2 their unbalance. It must be

$$m_{s1}e_1 + m_{s2}e_2 = me \tag{17}$$

This is the equilibrium of forces considering the two masses together. It is equivalent to the force equilibrium of the masses taken singularly, as no radial force is transmitted by the shaft; in this case, the inertia force of the single mass is supported by the correspondent bearing. The advantage of considering the mass concentrated in correspondence of bearings is that the stability of the single bearing can be evaluated separately, with a reduced number of DOFs.

$$\begin{bmatrix} m_{si} & 0 \\ 0 & m_{si} \end{bmatrix} \begin{bmatrix} \ddot{x}_C \\ \ddot{y}_C \end{bmatrix} + \begin{bmatrix} k_{xxi} & k_{xyi} \\ k_{yxi} & k_{yyi} \end{bmatrix} \begin{bmatrix} x_C \\ y_C \end{bmatrix} = \omega^2 m_{si} e_i \begin{bmatrix} \cos\omega t \\ \sin\omega t \end{bmatrix} \tag{18}$$

Conical whirl

Starting from system (3) and imposing the conical whirl it is.

$x_{C1} = \vartheta_y l_1; y_{C1} = -\vartheta_x l_1; x_{C2} = -\vartheta_y l_2; x_{C2} = -\vartheta_y l_2; y_{C2} = \vartheta_x l_2; e = 0$

As $\frac{x_{C1}}{l_1} = -\frac{x_{C2}}{l_2}$ some elements in the mass matrix are zeroed:

$$\begin{aligned} &\frac{1}{l_1+l_2}\begin{bmatrix} 0 & 0 & 0 & 0 \\ 0 & 0 & 0 & 0 \\ I & 0 & -I & 0 \\ 0 & I & 0 & -I \end{bmatrix} \begin{bmatrix} \ddot{x}_{C1} \\ \ddot{y}_{C1} \\ \ddot{x}_{C2} \\ \ddot{y}_{C2} \end{bmatrix} \\ &+ \frac{1}{l_1+l_2}\begin{bmatrix} 0 & 0 & 0 & 0 \\ 0 & 0 & 0 & 0 \\ 0 & I_p\omega & 0 & -I_p\omega \\ -I_p\omega & 0 & I_p\omega & 0 \end{bmatrix} \begin{bmatrix} \dot{x}_{C1} \\ \dot{y}_{C1} \\ \dot{x}_{C2} \\ \dot{y}_{C2} \end{bmatrix} \\ &+ \begin{bmatrix} k_{xx1} & k_{xy1} & k_{xx2} & k_{xy2} \\ k_{yx1} & k_{yy1} & k_{yx2} & k_{yy2} \\ k_{xx1}l_1 & k_{xy1}l_1 & -k_{xx2}l_2 & -k_{xy2}l_2 \\ k_{yx1}l_1 & k_{yy1}l_1 & -k_{yx2}l_2 & -k_{yy2}l_2 \end{bmatrix} \begin{bmatrix} x_{C1} \\ y_{C1} \\ x_{C2} \\ y_{C2} \end{bmatrix} \\ &= \omega^2 \begin{bmatrix} 0 \\ 0 \\ (I-I_p)\gamma\cos(\omega t+\varphi_1) \\ (I-I_p)\gamma\sin(\omega t+\varphi_1) \end{bmatrix} \end{aligned} \tag{19}$$

In case of symmetry ($k_{ij1} \approx k_{ij2}$ and $l_1 \approx l_2$, or more generally $k_{ij1}l_1 \approx k_{ij2}l_2$) the first two lines are zeroed and the system can be further simplified neglecting the Coriolis terms:

$$\begin{aligned} &\frac{1}{l_1+l_2}\begin{bmatrix} I & 0 & -I & 0 \\ 0 & I & 0 & -I \end{bmatrix} \begin{bmatrix} \ddot{x}_{C1} \\ \ddot{y}_{C1} \\ \ddot{x}_{C2} \\ \ddot{y}_{C2} \end{bmatrix} \\ &+ \begin{bmatrix} k_{xx1}l_1 & k_{xy1}l_1 & -k_{xx2}l_2 & -k_{xy2}l_2 \\ k_{yx1}l_1 & k_{yy1}l_1 & -k_{yx2}l_2 & -k_{yy2}l_2 \end{bmatrix} \begin{bmatrix} x_{C1} \\ y_{C1} \\ x_{C2} \\ y_{C2} \end{bmatrix} \\ &= \omega^2 (I-I_p)\gamma \begin{bmatrix} \cos(\omega t+\varphi_1) \\ \sin(\omega t+\varphi_1) \end{bmatrix} \end{aligned} \tag{20}$$

Substituting the expressions of masses m_{s1} and m_{s2} from Table 8 for conical whirl we obtain

$$\begin{aligned} &\begin{bmatrix} m_{s1}l_1 & 0 & -m_{s2}l_2 & 0 \\ 0 & m_{s1}l_1 & 0 & -m_{s2}l_2 \end{bmatrix} \begin{bmatrix} \ddot{x}_{C1} \\ \ddot{y}_{C1} \\ \ddot{x}_{C2} \\ \ddot{y}_{C2} \end{bmatrix} \\ &+ \begin{bmatrix} k_{xx1}l_1 & k_{xy1}l_1 & -k_{xx2}l_2 & -k_{xy2}l_2 \\ k_{yx1}l_1 & k_{yy1}l_1 & -k_{yx2}l_2 & -k_{yy2}l_2 \end{bmatrix} \begin{bmatrix} x_{C1} \\ y_{C1} \\ x_{C2} \\ y_{C2} \end{bmatrix} \\ &= (m_{s1}e_1l_1 - m_{s2}e_2l_2) \begin{bmatrix} \cos(\omega t+\varphi_1) \\ \sin(\omega t+\varphi_1) \end{bmatrix} \end{aligned} \tag{21}$$

where it is

$$(I-I_p)\gamma = (m_{s1}e_1l_1 - m_{s2}e_2l_2) \tag{22}$$

Equations 21 represent to the equilibrium of moments of the masses concentrated in correspondence of bearings. As before, the equilibrium can be written for the single mass taken separately as no radial force is transmitted by the shaft and the inertia force of each mass is balanced by the corresponding bearing. Dividing by the arm l_i, the moment equilibrium simplifies into a force equilibrium.

$$\begin{aligned} &\begin{bmatrix} m_{si}l_i & 0 \\ 0 & m_{si}l_i \end{bmatrix} \begin{bmatrix} \ddot{x}_{Ci} \\ \ddot{y}_{Ci} \end{bmatrix} + \begin{bmatrix} k_{xxi}l_i & k_{xyi}l_i \\ k_{yxi}l_i & k_{yyi}l_i \end{bmatrix} \begin{bmatrix} x_{Ci} \\ y_{Ci} \end{bmatrix} \\ &= m_{s1}e_1l_i \begin{bmatrix} \cos(\omega t+\varphi_1) \\ \sin(\omega t+\varphi_1) \end{bmatrix} \end{aligned} \tag{23}$$

Open Access This article is licensed under a Creative Commons Attribution 4.0 International License, which permits use, sharing, adaptation, distribution and reproduction in any

medium or format, as long as you give appropriate credit to the original author(s) and the source, provide a link to the Creative Commons licence, and indicate if changes were made. The images or other third party material in this article are included in the article's Creative Commons licence, unless indicated otherwise in a credit line to the material. If material is not included in the article's Creative Commons licence and your intended use is not permitted by statutory regulation or exceeds the permitted use, you will need to obtain permission directly from the copyright holder. To view a copy of this licence, visit http://creativecommons.org/licenses/by/4.0/.

References

1. Grassam NS, Powell JW, Tanner RI (1965) Gas lubricated bearings. J Appl Mech 32(3):718–718. https://doi.org/10.1115/1.3627307
2. Castelli V, Elrod HG (1965) Solution of the stability problem for 360 deg self-acting, gas-lubricated bearings. J Basic Eng 87(1):199–210. https://doi.org/10.1115/1.3650508
3. White JW, Nigam A (1980) A factored implicit scheme for the numerical solution of the reynolds equation at very low spacing. J Lubr Technol 102(1):80–85. https://doi.org/10.1115/1.3251442
4. Lund JW (1968) Calculation of stiffness and damping properties of gas bearings. J Lubr Technol 90(4):4
5. Lund JW (1967) A theoretical analysis of whirl instability and pneumatic hammer for a rigid rotor in pressurized gas journal bearings. J Lubr Technol. https://doi.org/10.1115/1.3616933
6. Waumans T, Reynaerts D, Al-Bender F (2009) On the design of high-speed miniature air bearings: dynamic stability, optimisation and experimental validation (Ontwerp van miniatuur luchtlagers voor hoge snelheden: dynamische stabiliteit, optimalisatie en experimentele validatie)
7. Lund JW (1965) The stability of an elastic rotor in journal bearings with flexible, damped supports. J Appl Mech 32(4):911–920. https://doi.org/10.1115/1.3627335
8. Lund JW (1987) Review of the concept of dynamic coefficients for fluid film journal bearings. J Tribol 109(1):37–41. https://doi.org/10.1115/1.3261324
9. Vleugels P, Waumans T, Peirs J, Al-Bender F, Reynaerts D (2006) High-speed bearings for micro gas turbines: stability analysis of foil bearings. J Micromechan Microeng 16(9):S282
10. von Osmanski S, Larsen JS, Santos IF (2020) Multi-domain stability and modal analysis applied to gas foil bearings: three approaches. J Sound Vib 472:115174. https://doi.org/10.1016/j.jsv.2020.115174
11. Zheng LW et al (2022) Stability analysis on gas-lubricated bearing for high speed cryogenic turbo-expander. IOP Conf Ser Mater Sci Eng 1240(1):012061. https://doi.org/10.1088/1757-899X/1240/1/012061
12. Schiffmann J (2015) Integrated design and multi-objective optimization of a single stage heat-pump turbocompressor. J Turbomach 137:071002. https://doi.org/10.1115/1.4029123
13. San Andrés L (2006) Hybrid flexure pivot-tilting pad gas bearings: analysis and experimental validation». J Tribol 128(3):551–558. https://doi.org/10.1115/1.2194918
14. Park J-K, Kim K-W (2004) Stability analyses and experiments of spindle system using new type of slot-restricted gas journal bearings. Tribol Int 37(6):6
15. Li W-L, Shen R-W (2009) Linear stability analysis of the herringbone groove journal bearings in microsystems: consideration of gas rarefaction effects. J Tribol 131:041705. https://doi.org/10.1115/1.3201872
16. Pal DK, Majumdar BC (1984) Stability analysis of externally-pressurized gas-lubricated porous bearings with journal rotation. Part 1 Cylindrical whirl. Tribol Int 17(2):83–91. https://doi.org/10.1016/0301-679X(84)90049-5
17. Pal DK, Majumdar BC (1984) Stability analysis of externally-pressurized gas-lubricated porous bearings with journal rotation Part 2. Conical whirl. Tribol Int 17(2):92–98. https://doi.org/10.1016/0301-679X(84)90050-1
18. Czolczynski K (1999) Rotordynamics of gas-lubricated journal bearing systems. Springer, Berlin
19. Czołczyński K, Marynowski K (1996) Stability of symmetrical rotor supported in flexibly mounted, self-acting gas journal bearings. Wear 194(1):190–197. https://doi.org/10.1016/0043-1648(95)06843-0
20. Schiffmann J, Spakovszky ZS (2012) Foil bearing design guidelines for improved stability. J Tribol 135:011103. https://doi.org/10.1115/1.4007759
21. Pan CH (1964) Mechanical technology Inc Latham NY., Spectral analysis of gas bearing systems for stability studies. Defense technical information center, 1964. [Online]. Disponibile su: https://books.google.it/books?id=gOPcPgAACAAJ
22. Adams ML, Padovan J (1981) Insights into linearized rotor dynamics. J Sound Vib 76(1):129–142. https://doi.org/10.1016/0022-460X(81)90296-0
23. Nabuurs M, Reynaerts D, Al-Bender F (2025) Tilting-pad gas bearings for high-speed applications: analysis, design and validation. PhD Thesis
24. Waumans T, Peirs J, Al-Bender F, Reynaerts D (2011) Aerodynamic journal bearing with a flexible, damped support operating at 7.2 million DN. J Micromech Microeng 21:10

Publisher's Note Springer Nature remains neutral with regard to jurisdictional claims in published maps and institutional affiliations.